

# Formation of Cu-supported mesoporous silicates and aluminosilicates and liquid-phase oxidation of benzene catalyzed by the Cu-mesoporous silicates and aluminosilicates

Junji Okamura, Satoru Nishiyama, Shigeru Tsuruya<sup>\*</sup>, Mitsuo Masai<sup>1</sup>

*Department of Chemical Science and Engineering, Faculty of Engineering, Kobe University, Nada, Kobe 657, Japan*

Received 10 February 1997; accepted 21 November 1997

## Abstract

Mesoporous silicates (MCM-41 and Al-containing MCM-41) were applied to catalyst supports for liquid-phase benzene oxidation paying attention to their remarkable features, such as large surface area, ordered mesopores and high thermal stability. The MCM-41-supported Cu catalysts were prepared by the method of impregnation (Cu/MCM-41) and ion-exchange treatment (Cu–Na · MCM-41, Cu–H · MCM-41). The liquid-phase oxygenation of benzene to phenol over the MCM-41-supported Cu catalysts was studied using molecular oxygen as an oxidant and ascorbic acid as a reducing reagent for the Cu species. The MCM-41-supported Cu catalysts, particularly the Cu ion-exchanged H · MCM-41 (Cu–H · MCM-41), were more active than the corresponding Cu catalysts supported on SiO<sub>2</sub>, TiO<sub>2</sub>, MgO, NaZSM-5, NaY, or KL zeolites. The accumulation of hydrogen peroxide (H<sub>2</sub>O<sub>2</sub>) was confirmed during the liquid-phase oxidation of benzene catalyzed by the Cu-supported MCM-41. © 1998 Elsevier Science B.V. All rights reserved.

*Keywords:* Cu ion-exchanged H · MCM-41; Oxidation; Benzene; Phenol; Ascorbic acid

## 1. Introduction

Porous inorganic materials, such as active charcoal, silica gel, zeolite and pillared clay, which have many micropores in their structures, have been studied on their characterization and utilized in a variety of fields including adsorbents, supports and catalysts etc., because of their multifunctional properties. Among the porous materials, various zeolites which are

crystalline aluminosilicates, particularly artificially synthesized zeolites [1], have been particularly interesting because they possess uniform micropores and have been studied for their functions as molecular sieve, selective adsorption–separation, catalysts, and supports. With the extended application of zeolites, zeolites with larger pores, such as aluminophosphate VPI-5 [2] with 12–13 Å pore diameters and galliumphosphates Cloverite [3] with 13–14 Å pore diameters, have been synthesized. Mesoporous silicate with a uniform pore of about 30 Å has been synthesized [4] by intercalating kanemite which has a layered structure with a surfactant, followed by the removal of the surfactant and

<sup>\*</sup> Corresponding author. Fax: +81-78-8031150.

<sup>1</sup> Present address: Department of Applied Physics and Chemistry, The Fukui University of Technology, Gakuen 3-6-1, Fukui, 910 Japan.

the bridging of the layers through calcination. This mesoporous material has been named [5] FSM-16 after the synthesis conditions were optimized. Mesoporous silicates/aluminosilicates, which were classified into three forms: MCM-41 (hexagonal), MCM-48 (cubic), and MCM-L (lamellar) based on the structure of their mesopores, have been obtained [6,7] by hydrothermal synthesis using a surfactant as an organic template. MCM-41 has been applied [8] as a support of Ni and Mo catalysts for the hydrocracking of oil components with the help of the larger pores of the mesoporous supports. The catalytic conversion of propene to gasoline components has been reported [9] using MCM-41 catalysts modified with platinum. The large pores of MCM-41 have caused the insertion of a heteropoly acid ( $\text{H}_3\text{PW}_{12}\text{O}_{40}$ ) into the inner surface [10] and the synthesis of Ru and Pt clusters by the bottle-in-ship method in the mesopores [11]. Attempts to insert elements, such as Ti [12], Fe [13], or Mn [14] into the MCM-41 framework have been recently reported, but the structural characterization of these synthesized mesopores materials is not yet clear.

In this study, MCM-41, one of the M41S series, was synthesized by reference to the hydrothermal synthetic method of ZSM-5 zeolite and tried as the support of Cu catalysts for liquid-phase benzene oxidation to phenol [15]. Cu species were supported on MCM-41 and Al-containing MCM-41 by impregnation and ion-exchange methods, respectively, to investigate the influence of the supported method of Cu. The catalytic activity of Cu-supported MCM-41 in the liquid-phase benzene oxidation to phenol was compared with those of the Cu catalysts supported on other oxides.

## 2. Experimental

### 2.1. Synthesis of MCM-41

An aqueous solution including  $\text{C}_{16}\text{H}_{33}^-$  ( $(\text{CH}_3)_3\text{N} \cdot \text{Br}$  (36.4 g (0.1 mol)),  $\text{H}_2\text{SO}_4$  (95%,

2.4 ml), and  $\text{H}_2\text{O}$  (280 ml (15.6 mol)) and an aqueous solution including  $\text{SiO}_2$  (51.8 g (0.25 mol)) and  $\text{H}_2\text{O}$  (133 ml (7.4 mol)) were dropwise poured into 213 ml (11.8 mol) of  $\text{H}_2\text{O}$  while stirring at room temperature and keeping the pH value of the mixed solution at 10–11. The whole mixture was transferred to an autoclave and hydrothermally treated ( $2.0 \text{ kg/cm}^2$ ) at 373 K for 30 h. After the resulting product was filtered off under vacuum, the product was washed with deionized hot water (333–343 K) until the filtrate became almost neutral. The hot water was used because of reducing the dissolved amount of  $\text{CO}_2$  and inhibiting the reaction of the unreacted material,  $\text{Na}_2\text{SiO}_3$ , with  $\text{H}_2\text{CO}_3$  to form amorphous  $\text{SiO}_2$ . The product was dried at 393 K for more than 12 h, followed by the removal of the organic template by calcining at 923 K for 1 h in a  $\text{N}_2$  flow and for 3 h in an air flow. The introduction of Al to MCM-41 to form  $\text{Na} \cdot \text{MCM-41}$  was performed adding the prescribed amount of  $\text{Al}_2(\text{SO}_4)_3 \cdot 18\text{H}_2\text{O}$  to solution A.  $\text{H} \cdot \text{MCM-41}$  was prepared by ion-exchanging the  $\text{Na}^+$  ions with the  $\text{H}^+$  ions. Thus,  $\text{Na} \cdot \text{MCM-41}$  was ion-exchanged with 1 N  $\text{NH}_4\text{NO}_3$  aqueous solution at 343–353 K for 6 h, which treatment was repeated three times. After the ion-exchange treatments, the MCM-41 was washed with deionized water, filtered off, dried at 393 K overnight, and calcined at 773 K for 5 h in an air flow.

### 2.2. Preparation of Cu-supported MCM-41 catalysts

Cu-impregnated MCM-41 (Cu/MCM-41) was prepared by impregnating the synthesized MCM-41 with an aqueous solution of a prescribed concentration of  $\text{Cu}(\text{CH}_3\text{COO})_2 \cdot \text{H}_2\text{O}$  followed by the evaporation of the solvent, drying at 393 K overnight, and calcination at 773 K for 5 h in an air flow. Cu ion-exchanged MCM-41 (Cu–Na · MCM-41, Cu–H · MCM-41) was prepared using Na · MCM-41 and H · MCM-41 (both the Si/Al atomic ratios, 55), which possess ion-exchangeable sites, as support. Each

support was ion-exchanged in an aqueous solution of a prescribed concentration of  $\text{Cu}(\text{CH}_3\text{COO})_2 \cdot \text{H}_2\text{O}$  at 353 K for 2 h. After filtering off and washing with deionized water, the resulting Cu ion-exchanged MCM-41 was dried overnight at 393 K, calcined at 773 K for 5 h in an air flow to prepare Cu–Na · MCM-41 and Cu–H · MCM-41. The Si/Al ratio of Na · MCM-41 and the amounts of ion-exchanged Cu of Cu–Na · MCM-41 and Cu–H · MCM-41 were analyzed by atomic absorption (AA) measurement (Shimadzu type AA-630-01). The sample was homogeneously dissolved by adding a few drops of hydrofluoric acid before transfer to the AA measurement.

### 2.3. Preparation of oxide-supported Cu catalysts

The oxide-supported Cu catalysts were prepared by impregnating with  $\text{Cu}(\text{CH}_3\text{COO})_2 \cdot \text{H}_2\text{O}$  (Nacalai Tesque, guaranteed reagent), drying at 393 K overnight, and calcining at 773 K for 5 h in air. The oxides used as supports were  $\text{SiO}_2$  (Davison, Grade 62),  $\gamma\text{-Al}_2\text{O}_3$  (JRC-ALO-4),  $\text{SiO}_2\text{-Al}_2\text{O}_3$  (JRC-SAL-2),  $\text{TiO}_2$  (JRC-TIO-1), and MgO (Nacalai Tesque, guaranteed reagent). Cu ion-exchanged zeolite catalysts were prepared by the conventional ion-exchange method at 353 K for 2 h using  $\text{Cu}(\text{CH}_3\text{COO})_2 \cdot \text{H}_2\text{O}$  (Nacalai Tesque, guaranteed reagent), washing with deionized water, filtering off, drying at 393 K overnight, and calcining at 773 K for 5 h in air. The zeolites used as supports were NaZSM-5 (Si/Al = 84, synthesized according to the literature [16]), KL (Si/Al = 3.4, Tosol), NaY (Si/Al = 2.8), and the H-type counterparts of NaZSM-5 and NaY. The H-type zeolites were prepared by ion-exchanging (three times) the Na-type zeolites with 1 N  $\text{NH}_4\text{NO}_3$  aqueous solution, washing with deionized water, filtering off, drying at 393 K overnight, and calcining at 773 K for 5 h. The amounts of ion-exchanged Cu were determined by AA measurement as previously described.

### 2.4. Measurement of X-ray diffraction (XRD)

The XRD patterns of the support and the catalyst samples were measured at room temperature by the Rigaku PMG-22 XRD equipment with an X-ray source of  $\text{CuK}\alpha$ .

### 2.5. Measurement of BET surface area

The surface areas of the supports and the catalysts were measured using a low-pressure static gas adsorption apparatus, based on the BET method [17] using the amount of  $\text{N}_2$  adsorption at 76 K. The samples were evacuated at 627 K for 1 h before the adsorption measurement.

### 2.6. Differential thermal (DTA) and thermal gravimetric (TG) analyses

The DTA and TG analyses of the uncalcined MCM-41 were performed using a Shimadzu type DTG-40 equipment with the rising temperature rate of 20 K/min.

### 2.7. Measurement of pore size distribution

The pore size distribution of the synthesized MCM-41 was obtained using an automatic surface area-pore size distribution measurement equipment (Carlo Erba type Sorptomatic 1800 series), applying the calculation of the B.J.H. method [18] to the adsorption–desorption isotherm of  $\text{N}_2$  at 76 K. The sample was evacuated at 523 K for 3 h.

### 2.8. Transmission electron (TEM) and scanning electron (SEM) microscopes

The TEM of MCM-41 was observed by a Hitachi type H-8100 TEM equipment operated at 200 kV, with 50,000 magnification. The SEM image of MCM-41 was observed by a Hitachi type S-4500 SEM equipment operated at 15–150 kV, with 5000–10 000 magnification. The sample was coated with Pt to prevent charge-up.

## 2.9. Liquid-phase oxidation of benzene

Benzene (Nacalai Tesque, guaranteed reagent) was checked by GLC and used without further purification. Ascorbic acid, 1 N acetic acid aqueous solution, methanol, ethanol, and 1-propanol were all purchased from Nacalai Tesque (guaranteed reagent). Oxygen and nitrogen gases (Kobe oxygen) were used as received. The liquid-phase oxidation of benzene was performed using a 50-cm<sup>3</sup> flask with a magnetic stirrer. The oxidation reaction was usually carried out under the following conditions: solvent, 20 cm<sup>3</sup> of 1 N acetic acid aqueous solution; catalyst, 0.40 g; reducing reagent, 4 mmol of ascorbic acid; oxygen atmosphere, 0.1 MPa; temperature, 303 K; reaction time, 5 h. After the separation of the catalyst by centrifugation, the analyses of the oxidation products were performed using a GLC (Shimadzu type GC-8A; detector, FID) with a 3-m stainless steel column (i.d., 3 mm) containing Silicon OV-17 (at 180°C, under N<sub>2</sub> carrier) and a 1.5-m stainless steel column (i.d., 3 mm) containing Thermon-3000 5% (Shincarbon A) (at 220°C, under N<sub>2</sub> carrier). The carbon balance was usually greater than 90%.

## 2.10. Quantitative analysis of hydrogen peroxide (H<sub>2</sub>O<sub>2</sub>)

After the oxidation reaction under the standard conditions previously described for the prescribed time, the catalyst was separated from the reaction solution by centrifugation. The amount of the accumulated H<sub>2</sub>O<sub>2</sub> during oxida-

tion was quantitatively analyzed by conventional iodometry [19].

## 3. Results and discussion

In this study, we synthesized MCM-41 by reference to the synthesis method of ZSM-5 zeolite [16], as described in Section 2. The XRD pattern of the white powder material obtained was a typical one of MCM-41 materials [20]. The synthesized MCM-41 was observed by TEM to directly confirm the presence of the hexagonal structure in the mesopore size [6,7,21–23]. The MCM-41 was found to have uniform mesopores of ca. 32 Å (cf., the observed value by TEM, ca. 30 Å). The BET surface area of the synthesized MCM-41 was 1052 m<sup>2</sup>/g. The pore volume calculated using the adsorption amount of N<sub>2</sub> at the saturated vapor pressure was 1.1 cm<sup>3</sup>/g. The MCM-41 synthesized in this study is heat resistant at least up to 1123 K. The physical properties of the MCM-41 and Al-containing MCM-41 (Na·MCM-41) obtained here are listed in Table 1.

### 3.1. Characterization of Cu-supported MCM-41

The variation of the powder XRD patterns of the Cu-impregnated MCM-41 (Cu/MCM-41) with the amount of the impregnated Cu is illustrated in Fig. 1. The impregnation of Cu on the MCM-41 support did not cause appreciable change in the XRD pattern, and the intensities of the (100) plane were almost constant, regardless of the amount of supported Cu. The BET

Table 1  
Physical properties of MCM-41 and Al-containing MCM-41 (Na·MCM-41)

| Mesoporous material | Si/Al atomic ratio |         | BET SA (m <sup>2</sup> /g) | Pore diameter (Å) | Pore volume (cm <sup>3</sup> /g) |
|---------------------|--------------------|---------|----------------------------|-------------------|----------------------------------|
|                     | Starting mixture   | Product |                            |                   |                                  |
| MCM-41              | —                  | —       | 1052                       | 31                | 1.1                              |
| Na·MCM-41           | 100                | 98      | 1054                       | 32                | 1.2                              |
|                     | 50                 | 55      | 1031                       | 32                | 1.2                              |
|                     | 25                 | 30      | 641                        | 30                | 1.1                              |

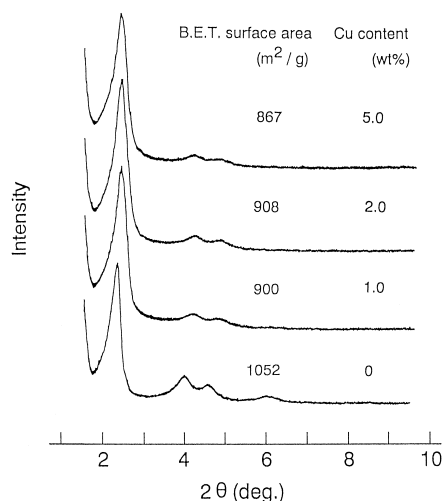


Fig. 1. Variation of XRD powder patterns of Cu-impregnated MCM-41 (Cu/MCM-41) with the amount of the supported Cu.

surface area decreased by supporting 1.0 wt.% of Cu on the MCM-41 by ca.  $150 \text{ m}^2/\text{g}$ , but the surface area did not decrease so much by an increase in the amount of supported Cu. The impregnation of Cu species on the MCM-41 was thus confirmed to preserve the hexagonal array and high surface area of MCM-41.

Fig. 2 shows the variation of the powder XRD pattern of the Cu ion-exchanged Na ·

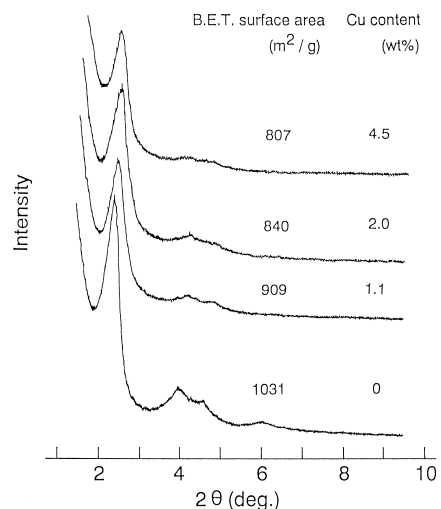


Fig. 2. Variation of XRD powder patterns of Cu ion-exchanged Na · MCM-41 (Cu–Na · MCM-41, Si/Al = 55) with the amount of the supported Cu.

MCM-41 (Cu–Na · MCM-41, Si/Al = 55), together with the BET surface area, with the amount (wt.%) of the ion-exchanged Cu. The variation of the XRD pattern was similar to that of the Cu/MCM-41 of which the Cu species was supported by impregnation method. Fig. 3 illustrates the variation of the powder XRD pattern of the Cu ion-exchanged H · MCM-41 (Cu–H · MCM-41, Si/Al = 55). The surface area considerably decreased by ion-exchanging Na in the Na · MCM-41 by a proton (surface areas of Na · MCM-41 and H · MCM-41 are 1031 and 856, respectively). The Cu ion-exchange in the H · MCM-41 support caused an appreciable decrease in the diffraction peaks at  $2\theta$  of ca.  $4\text{--}6^\circ$ , together with the decrease in surface area, in the range of the Cu amount of more than ca. 1 wt.%. Particularly, the peaks of planes (110) and (200) at a  $2\theta$  of ca.  $4^\circ$  almost disappeared when 2.0 and 4.6 wt.% of Cu were supported in the H · MCM-41, which results suggest a decrease in the hexagonal regularity of the structure. Luan et al. [24] have reported that the ion-exchange of Na in Na · MCM-41 with  $\text{NH}_4^+$  results in the removal of part of the Al atoms from the Na · MCM-41 followed by a

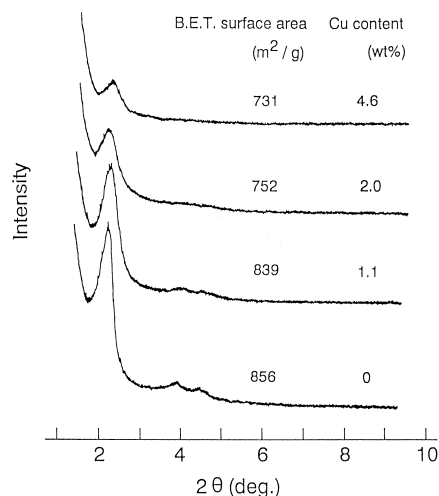


Fig. 3. Variation of XRD powder patterns of Cu ion-exchanged H · MCM-41 (Cu–H · MCM-41, Si/Al = 55) with the amount of the supported Cu.

weakness in the structural strength. Displacement of  $H^+$ , of which the radius is smaller than that of  $Na^+$ , has been reported [24] to cause the imbalance in the polarity of the structure, which imbalance results in the destruction of the uniform hexagonal structure. The ion-exchanges of  $Na^+$  in the  $Na \cdot MCM-41$  with  $H^+$  followed by  $Cu^{2+}$  in this study will also make the balance in the polarity change followed by the partial destruction of the regular hexagonal array, as shown in Fig. 3.

### 3.2. Cu species supported in MCM-41

The powder XRD patterns of  $Cu/MCM-41$ ,  $Cu \cdot NaMCM-41$ , and  $Cu \cdot H\text{MCM-41}$  in the region of  $2\theta$  of  $35\text{--}50^\circ$  were observed to investigate the dispersion states of Cu species supported in each MCM-41, together with that of Cu impregnated in  $SiO_2$  ( $Cu/SiO_2$ ), as shown in Fig. 4. The amount of Cu in all the samples was at an almost similar level (4.5–5.0 wt.%). The peaks based on CuO species were observed in the XRD of the  $Cu/MCM-41$  (Fig. 4c), together with the  $Cu/SiO_2$  (Fig. 4d). The half-height widths of the CuO peaks of the  $Cu/MCM-41$  were larger than those of the

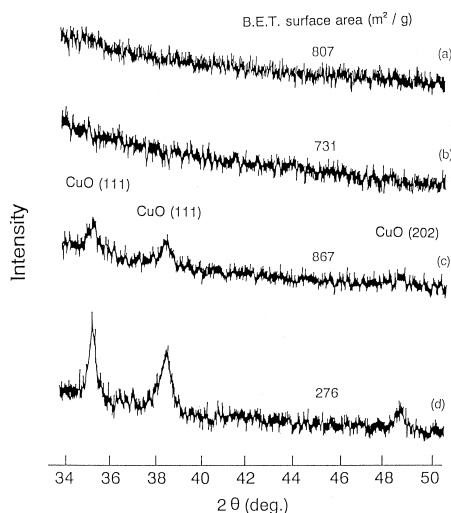


Fig. 4. XRD patterns of Cu species in Cu-supported MCM-41. (a)  $Cu(4.5)\text{-Na} \cdot MCM-41$ , (b)  $Cu(4.6)\text{-H} \cdot MCM-41$ , (c)  $Cu(5.0)/MCM-41$ , (d)  $Cu(5.0)/SiO_2$  ( $SiO_2$ , Davison).

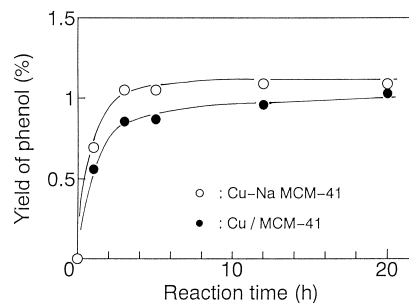


Fig. 5. Time dependence of phenol yield in benzene oxidation catalyzed by Cu-supported MCM-41. Reaction temperature, 303 K; benzene, 2 ml; solvent, 20 ml of 1 M acetic acid aqueous solution; reductant, 4 mmol of ascorbic acid; catalyst, 0.4 g; ●,  $Cu(1.0)/MCM-41$ ; ○,  $Cu(1.1)\text{-Na} \cdot MCM-41$ .

$Cu/SiO_2$  (the half-height width of  $CuO$  (111); 0.60 cm for the  $Cu/MCM-41$ , 0.33 cm for the  $Cu/SiO_2$ , the half-height width of  $CuO$  (111); 0.66 cm for the  $Cu/MCM-41$ , 0.60 cm for the  $Cu/SiO_2$ ). The results suggest that the particle size of  $CuO$  in the  $Cu/MCM-41$  is smaller than that in the  $Cu/SiO_2$ . In contrast to the Cu-supported catalysts ( $Cu/MCM-41$  and  $Cu/SiO_2$ ) prepared by the impregnation method, no diffraction peaks attributed to  $CuO$  (or  $Cu$ ,  $Cu_2O$ ) were detected in either the XRD of the  $Cu\text{-Na} \cdot MCM-41$  (Fig. 4a) or the  $Cu\text{-H} \cdot MCM-41$  (Fig. 4b), which suggests that the Cu species supported in  $Na \cdot MCM-41$  or  $H \cdot MCM-41$  by the ion-exchange method are present as  $Cu^{2+}$  and/or small particles of  $CuO$ . The uniform mesopores array and the high surface area specified to the MCM-41 structure will be attributed to the high dispersion of the supported Cu species.

### 3.3. Liquid-phase oxidation of benzene

The reaction product obtained in this study was only phenol, and no other product was detected. Fig. 5 illustrates the time dependence of the phenol yield at 303 K using  $Cu(1.0 \text{ wt.})/MCM-41$  and  $Cu(1.1 \text{ wt.})\text{-Na} \cdot MCM-41$  catalysts. The phenol yield increased with increasing reaction time up to the reaction

time of 3–5 h, but almost leveled off at a longer reaction time. The Cu–Na · MCM-41 was found to have larger catalytic activity for phenol formation than the Cu/MCM-41 catalyst.

The dependence of the phenol yield at the reaction time of 5 h on the reaction temperature was investigated using the Cu(1.0)/MCM-41 catalyst (Fig. 6). The phenol yield increased with the increase in the temperature up to ca. 303 K and reached a maximum at around 303 K. The decrease in the phenol yield with the increase in the reaction temperature may be caused by the decrease in the amount of the dissolved oxygen with increasing temperature and/or the consumption of ascorbic acid by its direct oxidation with the increase in the reaction temperature. In fact, the increase in the reaction temperature caused the color change of the reaction solution to dark yellow; this is due to the dehydroascorbic acid produced by the oxidation of ascorbic acid itself.

The influence of the amount of impregnated Cu on phenol yield (at 303 K and for 5 h) was investigated using the Cu/MCM-41 catalyst (Fig. 7). The phenol yield significantly increased with an increase in the amount of impregnated Cu up to the Cu amount of 1 wt.%, but further increase in the Cu amount inversely tended to make the phenol yield slightly decrease. The turnover number (Phenol/Cu ratio) monotonously decreased with the amount of impregnated Cu. The increase in the particle

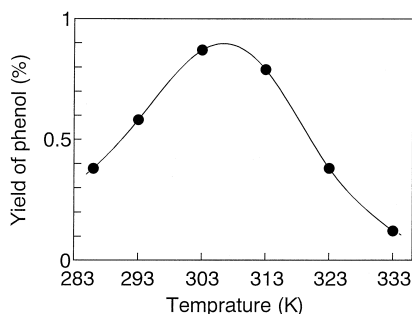


Fig. 6. Dependence of phenol yield on reaction temperature. Catalyst, 0.4 g of Cu(1.0)/MCM-41; reaction time, 5 h; benzene, 2 ml (22.5 mmol); solvent, 20 ml of 1 M acetic acid aqueous solution; reductant, 4 mmol of ascorbic acid.

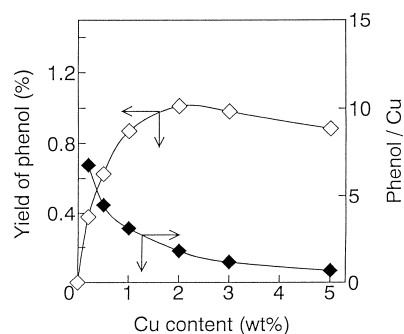


Fig. 7. Effect of Cu content impregnated on phenol yield. Catalyst, 0.4 g of Cu(1.0)/MCM-41; reaction time, 5 h; reaction temperature, 303 K; benzene, 2 ml (22.5 mmol); solvent, 20 ml of 1 M acetic acid aqueous solution; reductant, 4 mmol of ascorbic acid.

size of the Cu species like CuO with the increase in the amount of the impregnated Cu may be one of the causes of the decrease in the phenol yield with increasing impregnated Cu. Fig. 8 shows the effect of the amount of ion-exchanged Cu on the phenol yield using Cu–Na · MCM-41 and Cu–H · MCM-41 catalysts. Both catalysts were found to have similar catalytic behavior for benzene oxidation, though the Cu–H · MCM-41 catalyst had slightly greater catalytic activity than the Cu–Na · MCM-41. An increase in the amount of ion-exchanged Cu

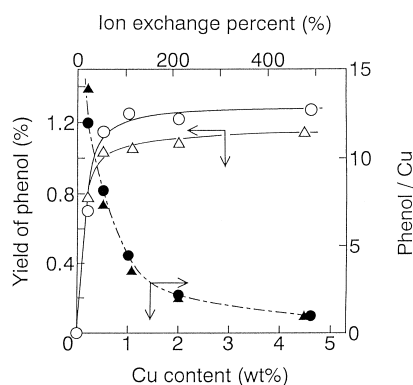


Fig. 8. Effect of Cu content ion-exchanged on phenol yield. Reaction time, 5 h; reaction temperature, 303 K; benzene, 2 ml (22.5 mmol); solvent, 20 ml of 1 M acetic acid aqueous solution; reductant, 4 mmol of ascorbic acid; phenol yield: ○, Cu–H · MCM-41; △, Cu–Na · MCM-41; phenol/Cu ratio: ●, Cu–H · MCM-41; ▲, Cu–Na · MCM-41.

caused the sharp increase in the phenol yield up to the Cu amount of ca. 1 wt.%. However, further increase in the Cu amount caused only a slight increase in the phenol yield. A comparison of Figs. 7 and 8 indicates that the Cu–Na · MCM-41 and Cu–H · MCM-41 catalysts have larger catalytic activities (larger turnover number) for benzene oxidation than the Cu/MCM-41 catalyst in the region of the supported Cu amount of less than 1 wt.%.

The results of the liquid-phase oxidation of benzene using Cu catalysts supported on the various amorphous and crystalline oxides by impregnation and ion-exchange methods, in addition to the MCM-41, are summarized in Table 2. Silica–alumina, alumina, and MCM-41 were found to be good supports among the oxides used as the support of Cu catalysts prepared by the impregnation method. Thus, in the case of the impregnated Cu catalysts, no superiority of MCM-41 as a support for benzene oxidation was found among the oxides studied. On the other hand, H · MCM-41 was the best support among the oxides used as the support of the Cu catalysts prepared by the ion-exchange method. It is of interest to note that regarding the Cu catalysts prepared by the ion-exchange method, the oxide support having a larger pore size

tended to have greater catalytic activity for benzene oxidation.

The scheme of benzene oxidation to phenol using a Cu catalyst has been considered [25–27] to be similar to the hydroxylation reaction by the Fenton reagent [28]. In the present oxidation system, both molecular oxygen as an oxidant and ascorbic acid as a reductant [29] were found to be necessary for phenol formation using the Cu/MCM-41 catalyst. In order to investigate whether H<sub>2</sub>O<sub>2</sub> as an intermediate is in fact formed during the benzene oxidation catalyzed by Cu(1.0)/MCM-41, the amount of H<sub>2</sub>O<sub>2</sub> accumulated during the benzene oxidation was quantitatively analyzed as illustrated in Fig. 9. H<sub>2</sub>O<sub>2</sub> was found to have accumulated during the benzene oxidation using the Cu/MCM-41 catalyst. The decrease in the amount of H<sub>2</sub>O<sub>2</sub> accumulated during the benzene oxidation at the reaction time of more than ca. 5 h may be due to the self-decomposition of H<sub>2</sub>O<sub>2</sub> on the Cu-supported catalyst. To investigate the participation of the hydroxy radical assumed to be formed by the decomposition of H<sub>2</sub>O<sub>2</sub> during the benzene oxidation, the effect of added alcohol, which is well known as a scavenger for the hydroxy radical, on phenol formation was investigated using 1-propanol, ethanol, and methanol

Table 2  
Benzene oxidation to phenol catalyzed by supported Cu catalysts

| Catalyst  | Cu content (wt.%) | Si/Al | BET SA (m <sup>2</sup> /g) |              | Support pore size (Å) | Yield of phenol (%) | Phenol/Cu ratio |
|---|-------------------|-------|----------------------------|--------------|-----------------------|---------------------|-----------------|
|   |                   |       | Support                    | Catalyst     |                       |                     |                 |
| Cu/TiO <sub>2</sub>                                 | 1.0               | —     | 73                         | 78           | —                     | 0.15                | 0.53            |
| Cu/MgO  | 1.0               | —     | <sup>a</sup>               | <sup>a</sup> | —                     | 0.58                | 2.1             |
| Cu/Al <sub>2</sub> O <sub>3</sub>                   | 1.0               | —     | 177                        | 162          | —                     | 0.90                | 3.2             |
| Cu/SiO <sub>2</sub> –Al <sub>2</sub> O <sub>3</sub> | 1.0               | 4.6   | 560                        | 432          | —                     | 0.96                | 3.5             |
| Cu/SiO <sub>2</sub>                                 | 1.0               | —     | 331                        | 276          | —                     | 0.77                | 2.8             |
| Cu/MCM-41   | 1.0               | —     | 1052                       | 900          | 31                    | 0.88                | 3.1             |
| Cu–NaZSM-5  | 1.1               | 84    | 355                        | 378          | 5.5                   | 0.74                | 2.4             |
| Cu–HZSM-5   | 0.9               | 84    | 404                        | 389          | 5.5                   | 0.39                | 1.5             |
| Cu–KL   | 1.2               | 3.4   | 323                        | 332          | 7.1                   | 0.96                | 2.9             |
| Cu–NaY  | 1.0               | 2.8   | 746                        | 627          | 7.4                   | 0.91                | 3.2             |
| Cu–HY   | 1.2               | 2.8   | 638                        | 607          | 7.4                   | 0.81                | 2.5             |
| Cu–Na · MCM-41                                      | 1.1               | 55    | 1031                       | 909          | 32                    | 1.1                 | 3.5             |
| Cu–H · MCM-41                                       | 1.1               | 55    | 856                        | 839          | 32                    | 1.3                 | 4.3             |

<sup>a</sup>Not measured.



as added alcohols. In the simplest form, if the hydroxy radical produced during the benzene oxidation is assumed to react with benzene and the added alcohol, the concentrations of the formed phenol and the added alcohol will be related according to following equation:

$$\frac{[\text{Phenol}]_0}{[\text{Phenol}]} = 1 + \frac{k_2[\text{Alcohol}]}{k_1[\text{Benzene}]}$$

where  $[\text{Phenol}]_0$  and  $[\text{Phenol}]$  are concentrations of phenol produced without and with the added alcohol, respectively.  $[\text{Benzene}]$  and  $[\text{Alcohol}]$  are concentrations of benzene and the added alcohol (these concentrations are assumed to be approximately constant);  $k_1$  and  $k_2$  are rate constants of the reactions between benzene and the hydroxy radical, and between alcohol and the hydroxy radical, respectively. The ratio  $[\text{Phenol}]_0/[\text{Phenol}]$  was plotted against  $[\text{Alcohol}]$  as shown in Fig. 10. Except for the region of small concentrations of the added alcohol, the plots were almost linear, regardless of the added alcohol. Thus, the participation of the hydroxy radical during the benzene oxidation catalyzed by Cu/MCM-41 is suggested. The extent of decrease in the phenol yield by adding alcohol was on the order of 1-propanol  $\geq$  ethanol  $>$  methanol. This order is thought to

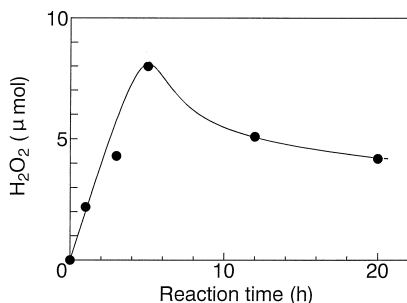


Fig. 9. Dependence of accumulated  $\text{H}_2\text{O}_2$  amount on reaction time. Catalyst, 0.4 g of Cu(1.0)/MCM-41; reaction temperature, 303 K; benzene, 2 ml (22.5 mmol); solvent, 20 ml of 1 M acetic acid; reductant, 4 mmol of ascorbic acid.

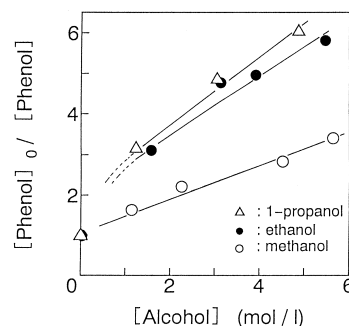


Fig. 10. Plots of ratio  $[\text{phenol}]_0/[\text{phenol}]$  against added alcohol concentration  $[\text{alcohol}]$ . Catalyst, 0.4 g of Cu(1.0)/MCM-41; reaction time, 5 h; reaction temperature, 303 K; benzene, 2 ml (22.5 mmol); solvent, 20 ml of 1 M acetic acid aqueous solution; reductant, 4 mmol of ascorbic acid; added alcohol: ○, methanol; ●, ethanol; △, 1-propanol.

be the order of the ability of the corresponding alcohol for scavenging the hydroxy radical.

#### 4. Conclusions

The Cu-supported MCM-41 (impregnation, Cu/MCM-41; ion-exchange; Cu-Na·MCM-41, Cu-H·MCM-41) was prepared using MCM-41 and Al-containing MCM-41 (Na·MCM-41, H·MCM-41) as supports by both the impregnation and ion-exchange methods. The mesoporous structure of MCM-41 was found to be almost maintained throughout the preparation of these Cu-supported MCM-41 catalysts. The Cu-supported MCM-41, together with the Cu catalysts supported in zeolites and amorphous oxides, were used as catalysts for the liquid-phase oxidation of benzene. The Cu ion-exchanged H·MCM-41 (Cu-H·MCM-41) had the highest catalytic activity for phenol formation among the catalysts in this study.  $\text{H}_2\text{O}_2$  was found to accumulate during the benzene oxidation catalyzed by the Cu-supported MCM-41.

#### Acknowledgements

Thanks are due to Dr. I. Kawafune of Osaka Municipal Technical Research Institute of In-

dustry for assistance with measurement of pore size distribution. Measurements of the TEM and SEM by Hitachi are gratefully acknowledged. The authors thank Mr. K. Nomura and Mr. T. Miyahara of Kobe University for their technical assistance and additional experiment during this work.

## References

- [1] R.M. Barrer, *J. Chem. Soc.* (1948) 2158.
- [2] M.E. Davis, C. Saldarriaga, C. Montes, J. Garces, C. Crowder, *Nature* 698 (1988) 331.
- [3] M. Estermann, L.B. McCusker, C. Baerlocher, A. Merrouche, H. Kessler, *Nature* 320 (1991) 352.
- [4] T. Yanagisawa, T. Shimizu, K. Kuroda, C. Kato, *Bull. Chem. Soc. Jpn.* 63 (1990) 988.
- [5] S. Inagaki, Y. Fukushima, K. Kuroda, *J. Chem. Soc., Chem. Commun.* (1993) 680.
- [6] C.T. Kresge, M.E. Leonowicz, W.J. Roth, J.C. Vartuli, J.S. Beck, *Nature* 359 (1992) 680.
- [7] J.S. Beck, J.C. Vartuli, W.J. Roth, M.E. Leonovicz, C.T. Kresge, K.D. Schmitt, C.T.W. Chu, D.H. Olson, E.W. Shepard, S.B. McCullen, J.B. Higgins, J.L. Schlenker, *J. Am. Chem. Soc.* 114 (1992) 10834.
- [8] A. Cosma, A. Martinez, V. Martinez-Soria, J.B. Monton, *J. Catal.* 153 (1995) 25.
- [9] T. Inui, J.B. Kim, M. Seno, *Catal. Lett.* 29 (1994) 271.
- [10] I.V. Kozhevnikov, A. Sinnema, R.J.J. Jansen, K. Pamin, H.V. Bekkum, *Catal. Lett.* 30 (1995) 241.
- [11] A.M. Liu, T. Shido, M. Ichikawa, *J. Chem. Soc., Chem. Commun.* (1995) 507.
- [12] T. Blasco, A. Corma, M.T. Navarro, J.P. Pariente, *J. Catal.* 156 (1995) 65.
- [13] Z.Y. Yuan, S.Q. Liu, T.H. Chen, J.Z. Wang, H.X. Li, *J. Chem. Soc., Chem. Commun.* (1995) 973.
- [14] D. Zhao, D. Goldfarb, *J. Chem. Soc., Chem. Commun.* (1995) 875.
- [15] T. Ohtani, S. Nishiyama, S. Tsuruya, M. Masai, *J. Catal.* 155 (1995) 158.
- [16] R.J. Araguier, G. Landolf, US Patent 3,702,886 (1989).
- [17] S. Brunauer, P.H. Emmett, E. Teller, *J. Am. Chem. Soc.* 60 (1938) 309.
- [18] E.P. Barrett, L.G. Joyner, P.P. Halenda, *J. Am. Chem. Soc.* 73 (1951) 373.
- [19] M. Ishibashi, Teiryō bunsemin jikken shishin, Toyama Shobou, 1965, p. 256.
- [20] R.J. Araguier, G. Landolf, US Patent 3,702,886 (1972).
- [21] J.C. Beck, C. Chu, I.D. Johnson, C.T. Kresge, M.E. Leonovicz, W.J. Roth, J.C. Vartuli, WO 9111390 (1991).
- [22] P.T. Tanev, M. Chibwe, T.J. Pinnavaia, *Nature* 368 (1994) 321.
- [23] P.J. Branton, P.G. Hall, K.S.W. Sing, H. Reichert, F. Schuth, K. Unger, *J. Chem. Soc., Faraday Trans.* 90 (1994) 2965.
- [24] Z. Luan, H. He, W. Zhou, C.F. Cheng, J. Klinowski, *J. Chem. Soc., Faraday Trans.* 91 (1995) 2955.
- [25] A. Kunai, S. Hata, S. Ito, K. Sasaki, *J. Am. Chem. Soc.* 108 (1986) 6012.
- [26] A. Kunai, S. Hata, S. Ito, K. Sasaki, *J. Org. Chem.* 51 (1986) 3471.
- [27] S. Ito, T. Yamazaki, H. Okada, S. Okino, K. Sasaki, *J. Chem. Soc., Perkin Trans.* 2 (1988) 285.
- [28] J.R.L. Smith, R.O.C. Norman, *J. Chem. Soc.* (1963) 2897.
- [29] M.M. Taquikhan, A.E. Martell, *J. Am. Chem. Soc.* 86 (1967) 4176.